

REPORT DOCUMENTATION PAGE			Form Approved OMB NO. 0704-0188		
<p>The public reporting burden for this collection of information is estimated to average 1 hour per response, including the time for reviewing instructions, searching existing data sources, gathering and maintaining the data needed, and completing and reviewing the collection of information. Send comments regarding this burden estimate or any other aspect of this collection of information, including suggestions for reducing this burden, to Washington Headquarters Services, Directorate for Information Operations and Reports, 1215 Jefferson Davis Highway, Suite 1204, Arlington VA, 22202-4302. Respondents should be aware that notwithstanding any other provision of law, no person shall be subject to any penalty for failing to comply with a collection of information if it does not display a currently valid OMB control number.</p> <p>PLEASE DO NOT RETURN YOUR FORM TO THE ABOVE ADDRESS.</p>					
1. REPORT DATE (DD-MM-YYYY) 23-01-2015		2. REPORT TYPE Final Report		3. DATES COVERED (From - To) 18-May-2011 - 17-May-2014	
4. TITLE AND SUBTITLE Final Report: Development of Novel Magnetic Metal Oxide Films and Carbon Nanotube Materials for Magnetic Device Applications			5a. CONTRACT NUMBER W911NF-11-1-0187		
			5b. GRANT NUMBER		
			5c. PROGRAM ELEMENT NUMBER 206022		
6. AUTHORS Keith Jackson, Conrad Williams, Dereje Seifu, Ezana Negresse			5d. PROJECT NUMBER		
			5e. TASK NUMBER		
			5f. WORK UNIT NUMBER		
7. PERFORMING ORGANIZATION NAMES AND ADDRESSES Morgan State University Civil Engineering 1700 E. Cold Spring Lane Baltimore, MD 21251 -0001			8. PERFORMING ORGANIZATION REPORT NUMBER		
9. SPONSORING/MONITORING AGENCY NAME(S) AND ADDRESS (ES) U.S. Army Research Office P.O. Box 12211 Research Triangle Park, NC 27709-2211			10. SPONSOR/MONITOR'S ACRONYM(S) ARO		
			11. SPONSOR/MONITOR'S REPORT NUMBER(S) 58961-MS-REP.3		
12. DISTRIBUTION AVAILABILITY STATEMENT Approved for Public Release; Distribution Unlimited					
13. SUPPLEMENTARY NOTES The views, opinions and/or findings contained in this report are those of the author(s) and should not be construed as an official Department of the Army position, policy or decision, unless so designated by other documentation.					
14. ABSTRACT Earlier wereport the successful fabrication of out-of-plane exchange spring in sputter deposited CoFe ₂ O ₄ /CoFe ₂ /CoFe ₂ O ₄ structures. Synthesis of the 5 ferrimagnetic hard layer CoFe ₂ O ₄ in oxygen-assisted environment contributed to the much larger coercive field in cobalt ferrite thin films. These results obtained in sputter-deposited CoFe ₂ O ₄ /CoFe ₂ samples are consistent with earlier work done on samples prepared with PLD (pulsed laser deposition). Recoil curves measurements done on samples with					
15. SUBJECT TERMS Nanomagnetics, carbon nanotubes, multilayer materials, spin springs, CoFe ₂ O ₄ films					
16. SECURITY CLASSIFICATION OF:			17. LIMITATION OF ABSTRACT	15. NUMBER OF PAGES	19a. NAME OF RESPONSIBLE PERSON
a. REPORT UU	b. ABSTRACT UU	c. THIS PAGE UU	UU		Keith Jackson
					19b. TELEPHONE NUMBER 443-885-3124

Report Title

Final Report: Development of Novel Magnetic Metal Oxide Films and Carbon Nanotube Materials for Magnetic Device Applications

ABSTRACT

Earlier we reported the successful fabrication of out-of-plane exchange spring in sputter deposited CoFe₂O₄/CoFe₂/CoFe₂O₄ structures. Synthesis of the 5 ferrimagnetic hard layer CoFe₂O₄ in oxygen-assisted environment contributed to the much larger coercive field in cobalt ferrite thin films. These results obtained in sputter-deposited CoFe₂O₄/CoFe₂ samples are consistent with earlier work done on samples prepared with PLD (pulsed laser deposition). Recoil curve measurements done on samples with 10 improved coercive field showed much reduced energy loss indicating higher degree of exchange spring. As indicated by the normalized area of the recoil curve, a measure of the degree of exchange spring, we observe that our systems begin to nucleate before the field of irreversible switching, H_{irr} is reached. This suggests, especially for in-plane configuration, most of the moments of the soft magnetic layer are recovering their original 15 orientation. The decrease in the moment during recoil measurement can be reduced by introducing a preferred orientation for the moments in the soft magnetic layer. Preliminary results show that by applying magnetic field during deposition and annealing, we can induce magnetic anisotropy and enhance the coupling between the soft and hard magnetic layers improving the exchange spring. We would also like to report on low 20 temperature magnetization and torque studies on our tri-layered Spin Spring Films. In order to enhance the observed spin effect, we extended the spin spring investigation to include multiple tri layers of CoFe₂O₄/CoFe₂/CoFe₂O₄ structures,

3

FINAL REPORT_v0, January 22, 2015 3 of 28

However, these studies have been significantly delayed because of the amount of time required to deposit just two CoFe₂O₄/CoFe₂/CoFe₂O₄ structures without breaking the vacuum by a combination of magnetron sputtering for the cobalt iron 25 (metal) and the inordinate amount of time required to RF sputter the cobalt-ferrite. We have chosen to take a new approach. The new approach entails using our UHV Pulsed Laser Deposition System to deposit the cobalt ferrite and modify the system to accommodate a magnetron attach sputtering gun to deposit the cobalt iron. This modification cost around \$50,000.

30 Recently we received all of the pieces to modify the system and making the installations in spite of the absence of addition funding from this grant.

During the interim we pursued the proposed nanowire studies on nanowire of Fe/NWCNTS/SiO₂ and nano films of Fe on MgO. From these studies we learned that nano wires of Fe grown in the lumens of multi-walled carbon nanotubes (MWCNTs) required four times higher 35 magnetic field strength to reach saturation compared to planar Fe nanometric thin films of Fe on MgO(100). Nanowires of Fe and nanometric films of Fe both exhibited two fold magnetic symmetries. Structural and magnetic properties of 1D nanowires and 2D nanometric films were studied by several magnetometry techniques. The θ -2 θ x-ray diffraction measurements showed that a secondary (200) peak of Fe appeared on thin film 40 samples deposited at higher substrate temperatures. In these samples prepared at higher temperatures lower coercive field and highly pronounced two-fold magnetic symmetry were observed.

Enter List of papers submitted or published that acknowledge ARO support from the start of the project to the date of this printing. List the papers, including journal references, in the following categories:

(a) Papers published in peer-reviewed journals (N/A for none)

<u>Received</u>	<u>Paper</u>
-----------------	--------------

TOTAL:

Number of Papers published in peer-reviewed journals:

(b) Papers published in non-peer-reviewed journals (N/A for none)

<u>Received</u>	<u>Paper</u>
-----------------	--------------

TOTAL:

Number of Papers published in non peer-reviewed journals:

(c) Presentations

Vancouver Dr. Williams
Japan Invited Talk Dr. Williams
Number of Presentations: 1.00

Non Peer-Reviewed Conference Proceeding publications (other than abstracts):

<u>Received</u>	<u>Paper</u>
-----------------	--------------

TOTAL:

Number of Non Peer-Reviewed Conference Proceeding publications (other than abstracts):

Peer-Reviewed Conference Proceeding publications (other than abstracts):

<u>Received</u>	<u>Paper</u>
01/23/2015	2.00 Korey Pough , Abebe Kebede, Dereje Seifu, Destenie Knock . Magnetic Properties of Iron Chalcogenide Superconducting Materials for Energy Storage Applications, March Meeting American Physical Society. 21-MAR-13, . : ,
TOTAL:	1

Number of Peer-Reviewed Conference Proceeding publications (other than abstracts):

(d) Manuscripts

<u>Received</u>	<u>Paper</u>
TOTAL:	

Number of Manuscripts:

Books

<u>Received</u>	<u>Book</u>
TOTAL:	

Received

Book Chapter

TOTAL:

Patents Submitted

Patents Awarded

Awards

Graduate Students

NAME

PERCENT SUPPORTED

FTE Equivalent:

Total Number:

Names of Post Doctorates

NAME

PERCENT SUPPORTED

Ezana Negresse

1.00

FTE Equivalent:

1.00

Total Number:

1

Names of Faculty Supported

NAME

PERCENT SUPPORTED

National Academy Member

Keith Jackson

0.00

Conrad Williams

0.00

Dereje Seifu

0.00

FTE Equivalent:

0.00

Total Number:

3

Names of Under Graduate students supported

<u>NAME</u>	<u>PERCENT SUPPORTED</u>	Discipline
Jamine Arribas	0.00	Physics
Dominic Smith	0.00	Electrical Engineering
Keion Howard	0.00	Physics
FTE Equivalent:	0.00	
Total Number:	3	

Student Metrics

This section only applies to graduating undergraduates supported by this agreement in this reporting period

The number of undergraduates funded by this agreement who graduated during this period: 1.00

The number of undergraduates funded by this agreement who graduated during this period with a degree in science, mathematics, engineering, or technology fields:..... 1.00

The number of undergraduates funded by your agreement who graduated during this period and will continue to pursue a graduate or Ph.D. degree in science, mathematics, engineering, or technology fields:..... 1.00

Number of graduating undergraduates who achieved a 3.5 GPA to 4.0 (4.0 max scale):..... 1.00

Number of graduating undergraduates funded by a DoD funded Center of Excellence grant for Education, Research and Engineering:..... 0.00

The number of undergraduates funded by your agreement who graduated during this period and intend to work for the Department of Defense 0.00

The number of undergraduates funded by your agreement who graduated during this period and will receive scholarships or fellowships for further studies in science, mathematics, engineering or technology fields:..... 1.00

Names of Personnel receiving masters degrees

<u>NAME</u>
Total Number:

Names of personnel receiving PHDs

<u>NAME</u>
Not applicable
Total Number:

Names of other research staff

<u>NAME</u>	<u>PERCENT SUPPORTED</u>
FTE Equivalent:	
Total Number:	

Sub Contractors (DD882)

Inventions (DD882)

Scientific Progress

See Attachment

Technology Transfer

TABLE OF CONTENT

	Progress Report for August 1, 2011 – July 31, 2014	2
1	Abstract	2
2	Activities	4
5	3 Scientific and technical progress	5
	3.1 Spin Spring Discussion	5
	3.1.1 Experimental	6
	3.1.2 Results and Discussion.....	9
	3.1.3 REPORT ON LOW TEMPERATURE STUDIES	13
10	3.1.4 REPORT ON THE IMPACT OF NEW INSTRUMENTATION	13
	3.1.5 Summary	13
	3.1.6 References	14
	3.2 Fe/NWCNTS/SiO ₂ and Nano Films of Fe on MgO.....	15
	3.2.1 Introduction	15
15	3.2.2 Experiment	17
	3.2.3 Results and Discussions	18
	3.2.4 Conclusion.....	20
	3.2.5 References	22
	4 Student Contributions.....	25
20	4.1 Jaime Arribas.....	26
	4.2 Dominic Smith	27
	4.3 Keion Howard	27
	4.4 Impact of the experience on the students	27

Progress Report for August 1, 2011 – July 31, 2014

Period covered by report: Beginning August 1, 2011 and ending July 31, 2014
Proposal Title: Development of Novel Magnetic Metal Oxide Thin Film and Carbon Nanotube Materials for Magnetic Device Applications
Contract Grant Number: W911NF-11-1-0187
Author of Report: Dr. Keith H. Jackson
Performing Organization: Morgan State University,
Name and Address: 1700 E. Cold Spring Lane, Baltimore, MD, 21251
ARO Proposal Number: 58961-MS-REP

1 Abstract

Earlier wereport the successful fabrication of out-of-plane exchange spring in
 5 sputter deposited $\text{CoFe}_2\text{O}_4/\text{CoFe}_2/\text{CoFe}_2\text{O}_4$ structures. Synthesis of the ferrimagnetic hard
 layer CoFe_2O_4 inoxygen-assisted environment contributed to the much larger coercive
 field in cobalt ferrite thin films. These results obtained in sputter-deposited
 $\text{CoFe}_2\text{O}_4/\text{CoFe}_2$ samples are consistent with earlier work done on samples prepared with
 PLD (pulsed laser deposition). Recoil curvesmeasurements done on samples with
 10 improved coercive field showed much reduced energy loss indicating higher degree of
 exchange spring. As indicated by the normalized area of the recoil curve, a measure of
 the degree of exchange spring, we observe that our systems begin to nucleate before the
 field of irreversible switching, H_{irr} is reached. This suggests, especiallyfor in-plane
 configuration,most of the moments of the soft magnetic layer are recovering their original
 15 orientation. Thedecreasein the moment during recoil measurement can be reduced by
 introducing a preferred orientation for the moments in the soft magnetic layer.
 Preliminary results show that by applying magnetic field during deposition and annealing,
 we can induce magnetic anisotropy and enhance the coupling between the soft and hard
 magnetic layers improving the exchange spring. We would also like to report on low
 20 temperature magnetization and torque studies on out tri-layered Spin Spring Films.

In order to enhance the observed spin effect, we extended the spin spring
 investigation to include multiple tri layers of $\text{CoFe}_2\text{O}_4/\text{CoFe}_2/\text{CoFe}_2\text{O}_4$ structures,

However, these studies have been significantly delayed because of the amount of time required to deposit just two $\text{CoFe}_2\text{O}_4/\text{CoFe}_2/\text{CoFe}_2\text{O}_4$ structures without breaking the vacuum by a combination of magnetron sputtering for the cobalt iron (metal) and the inordinate amount of time required to RF sputter the cobalt-ferrite. We have chosen to take a new approach. The new approach entails using our UHV Pulsed Laser Deposition System to deposit the cobalt ferrite and modify the system to accommodate a magnetron attach sputtering gun to deposit the cobalt iron. This modification cost around \$50,000. Recently we received all of the pieces to modify the system and making the installations in spite of the absence of addition funding from this grant.

During the interim we pursued the proposed nanowire studies on nanowire of Fe/NWCNTS/ SiO_2 and nano films of Fe on MgO. From these studies we learned that nano wires of Fe grown in the lumens of multi-walled carbon nanotubes (MWCNTs) required four times higher magnetic field strength to reach saturation compared to planar Fe nanometric thin films of Fe on MgO(100). Nanowires of Fe and nanometric films of Fe both exhibited two fold magnetic symmetries. Structural and magnetic properties of 1D nanowires and 2D nanometric films were studied by several magnetometry techniques. The θ -2 θ x-ray diffraction measurements showed that a secondary (200) peak of Fe appeared on thin film samples deposited at higher substrate temperatures. In these samples prepared at higher temperatures lower coercive field and highly pronounced two-fold magnetic symmetry were observed.

Keywords: Coercivity, Nanowire, Exchange Spring, Spin Spring

2 Activities

Submission or publication under ARO sponsorship:

Papers published in peer-reviewed journals: none

Papers published in non-peer-reviewed journals: none

Presentations:

Vancouver Dr. Williams

Japan Invited Talk Dr. Williams

Conferences Attended

APS Dr. Jackson, Dr. Williams and Dr. Seifu

(<http://meeting.aps.org/Meeting/MAR13/Session/V1.151>)

BNL Dr. Seifu

http://www.google.com/url?sa=t&rct=j&q=&esrc=s&source=web&cd=3&ved=0CDUQFjAC&url=http%3A%2F%2Fwww.bnl.gov%2Foaworkshop%2Fattendeess.php%3Fpageno%3D2&ei=ihA9UpUm6OXgA_6KgNgO&usq=AFQjCNH9zwLuX67i7ffs7oWXZxFJfuH-iA&bvm=bv.52434380,d.dmg

Student/Support Personnel Metrics

Graduate students: none

Post Doctorates: 1 FTE

Faculty: none

Undergraduate students: Jaime Arribas, Dominic Smith and Keion Howard

Masters Degrees Awarded: none

Ph.D.s Awarded: none

Other Research Staff: none

Technology Transfer: none

3 Scientific and technical progress

3.1 Spin Spring Discussion

With uniquely high moment, the family of insulating ferrites has renewed interest in complex oxides for numerous applications that take advantage of both charge and spin degree of freedom. With its high Curie temperature of 793 K [1], CoFe_2O_4 (CFO) has made room temperature spin filters that utilize spin tunneling possible. This has immense implications to the density and capacity of tunneling magnetoresistance (TMR) based systems. Advances in fabrication and characterization techniques have made this material accessible for both application and pure scientific investigation of new phenomena.

Previously, the application of CFO was mainly limited to a pinning layer in spin valves and other applications. Now, it is being pursued for other functions in addition to spin filtering. One such purpose is exchange spring systems due to its high coercive field. As Kneller and Hawig proposed [2], by interspersing hard and soft magnetic materials, both the coercive field and remnant magnetization of multilayer heterostructure can be engineered for specific purposes. It has been found that the magnetic properties of CFO are sensitive to the growth conditions making it an ideal model system.

In this study, we chose CoFe_2 as the soft magnetic layer because it has one of the highest remnant magnetic moment and it is of the same species as CFO (CoFe_2O_4). The choice of CoFe_2 eliminates complications that often arise in structures comprised of different species, due to interdiffusion of different species from one layer to the other at the interface decreasing the overall performance of the entire structure. The choice of this combination of CFO and CoFe_2 is designed to minimize the effect of inter-diffusion.

The two important metrics that determine the degree of exchange spring are coercive field (H_C) and the remnant magnetization (M_r). The hard and soft magnetic layers are selected because of their contribution to H_C and M_r , respectively. In this part of the study, our focus was on improving the coercive field of the CFO so as to enhance the exchange spring of the CoFe_2 and CFO system. To obtain optimum operating parameters for our sputtering deposition system, we systematically explored the important

parameters that affect the quality and magnetic properties of the deposited CFO film through several iterations where all but one parameter are kept constant. During a given iteration, a selected parameter is systematically varied and its impact on the magnetic properties of the sample carefully examined. These parameters include substrate temperature, deposition pressure, RF source's power, and ratio of Ar to O₂.

3.1.1 Experimental

The first structure we examined was a basic bilayer system composed of a thin film of CoFe₂O₄ as the hard magnetic layer and CoFe₂ as the soft magnetic layer. The 200 Å of soft magnetic layer was deposited using DC magnetron source from a 2 inch diameter and 1/16th inch thick CoFe₂ target at deposition rate of 0.5 Å/sec. Thinner targets are preferred because the strong magnetic field generated by the thicker target tends to shunt the plasma containing field of the sputtering source. In the instances where oxygen gas was introduced to the chamber, the CoFe₂ source is flushed by running it with higher Ar pressure (25 mTorr). Then before opening the shutter to begin deposition of CoFe₂, the pressure is lowered to 5 mTorr and the chamber is purged for about 6 to 14 minutes to ensure the metallic layer is deposited in oxygen free environment.

For depositing the 1000 Å thick CoFe₂O₄ layer from the RF source, the optimal settings were 120 W at 5 mTorr and 4.2 sccm of Ar yielding deposition rate of 4 Å/min. Such slower deposition rates are common in complex insulating oxides with high heat of formation. Raising the power to increase the deposition rate resulted in overheating the source. The gain obtained in the deposition rate was, however, significantly diminished when the power was increased beyond 160 W. A much preferred alternative approach is decreasing the Ar partial pressure in the chamber [3]. Decreasing the pressure below 2 mTorr was beyond the mass flow regulator's range, which in turn affected the plasma's stability in the chamber. Thus, the gain achieved may be at the expense of the consistency of the deposited film.

The impact of introducing oxygen gas in the chamber on the coercive field was substantial and striking. Adding oxygen during deposition nearly doubled the coercive field of the 2000 Å CoFe₂O₄ layer. This approach of adding oxygen is common practice

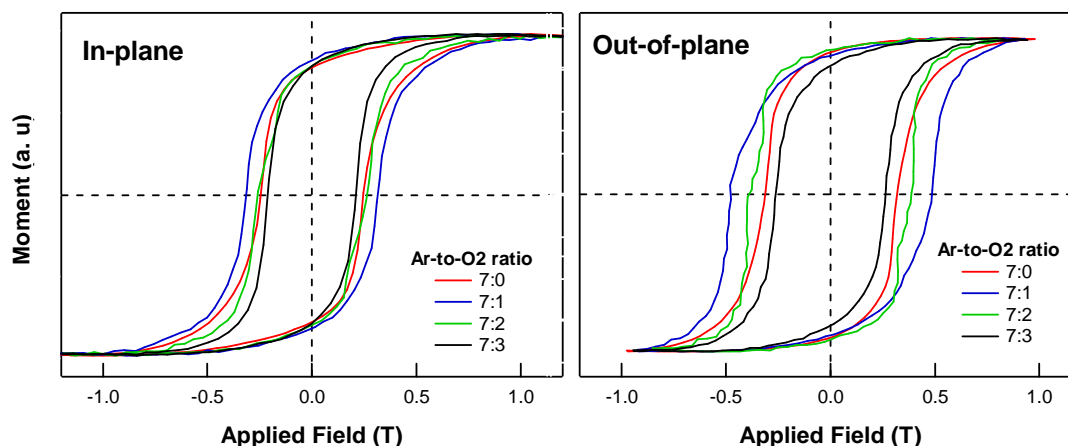


Fig.1: Room temperature hysteresis loops at different oxygen concentration. For both in-plane and out of plane configurations, the ratio of 7:1 yielded the largest increase in coercivity

[3, 4]; what makes this result remarkable is the degree to which it enhanced the coercive field from 2.2 to 3.1 kOe for in-plane and from 2.9 to 4.9 kOe for out-of-plane orientations. Lee and colleagues [7] reported out-of-plane coercive field of CFO deposited at 400°C was 1.5 kOe and it went up to 3.9 kOe after annealing at 500°C. Zhou *et.al.* also reported coercive field values of 1.8 to 2.0 kOe for their PLD deposited samples [5]. Similarly, Reghunathan *et al.* also reported coercivity of about 2.0 kOe [6]. We found that adding of oxygen during the deposition was far more consequential than substrate temperature, annealing temperature or annealing period [7, 8].

Shown in **Fig.1** are the in-plane and out-of-plane room temperature hysteresis loops of samples prepared with 7:0, 7:1, 7:2 and 7:3 Ar-to-O₂ ratios. The 7:1 ratio of Ar-to-O₂ resulted in higher coercive field, compared to the no oxygen or over-abundance of oxygen. As can be inferred from the graphs, over-abundance of oxygen diminishes the coercive field of the hard magnetic layer more than the deficiency of O₂. As shown in **Fig.1**, adding oxygen at the optimal ration of 7-to-1 resulted in an enhanced coercive field. The supplemental oxygen gas replenishes the oxygen that may have dissociated from the target and escaped because oxygen is a lighter element. This in turn improved exchange spring response in the trilayer.

The exchange spring response of a given system is measured using the measurement scheme outlined below. A typical recoil curve is shown in **Fig. 2** of a

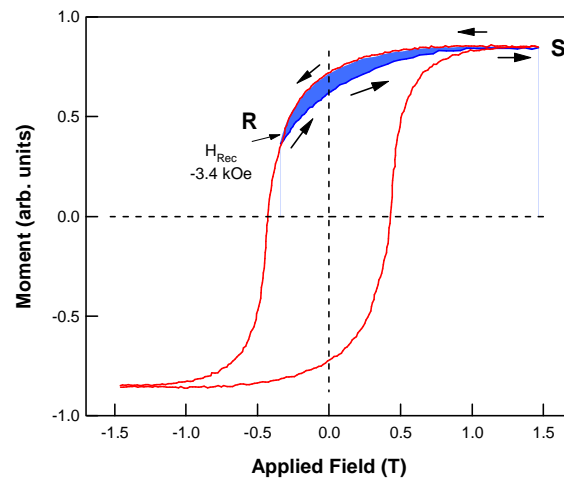


Fig. 2: Recoil curve measurement and recoil curve area

trilayer comprised of a 200 Å CoFe₂, a soft ferromagnetic material sandwiched by two 1000 Å CFO thick hard magnetic layer. The saturation field position, point S in **Fig. 2**, marks the field value at which all the moments are aligned in one direction by applying a sufficiently strong magnetic field, whereas point R (recoil position) marks the field at which the external applied magnetic field is reversed and swept back to point S. Initially, as the field is changed from point S to point R, the magnetization follows the path defined by the major hysteresis loop (solid red line in **Fig. 2**). For an ideal system, in the return path (from point R back to point S), the magnetization retraces the initial path (from point S to point R) displaying a perfect unwinding of the spring.

A deviation from the return path indicates a loss in the energy due to relaxation of the moments from their initial orientation. The loss in energy during recoil curve measurement can be determined by calculating the area under the curve. Dividing the area of the recoil curve by total energy of the system, represented by the maximum energy product (BH_{MAX}) hysteresis loop, gives the normalized recoil area. This *normalized recoil* area gives the fraction of the moments that relaxed and did not maintain their orientation and thus provides a direct measure of the degree of exchange spring of the system.

In our CFO/CoFe₂ bilayer samples, we observed the two phase system that typifies the weakly exchange coupled layers [9]. To enhance the coupling and improve

the exchange spring effect, a third CFO layer was added on top of the soft layer to take advantage of the available surface where the CoFe_2 layer can be exchange coupled to another hard magnetic layer. This top CFO layer also serves to reduce further oxidation of the metallic soft layer. Sandwiching the soft magnetic layer between two hard magnetic layers from both sides provides more interfacial contact strengthening the exchange spring effect [2].

3.1.2 Results and Discussion

Therecoil curves and the normalized area of a $\text{CoFe}_2\text{O}_4/\text{CoFe}_2/\text{CoFe}_2\text{O}_4$ trilayer deposited on silicon at 400°C with 7-to-1 Ar to O_2 ratio is shown in **Fig. 3**. As the recoil field exceeds the irreversible field value (H_{irr}), the exchange spring response is lost due to total switching of the hard layer. This critical field of irreversible response may occur before or after the coercive field for the given system.

Recoil curves and the fraction of normalized recoil curve areas are shown in the figure below (**Fig. 3**) for different recoil field settings. We find that recoil curve done in the out-of-plane orientation show higher degree of exchange spring as indicated by the smaller normalized recoil curve areas. For instance, at the recoil field value of -2.6 kOe, the fraction of normalized area is smaller in the out-of-plane configuration than that of the in-plane. The enhanced coercive field in out-of-plane orientation is responsible for

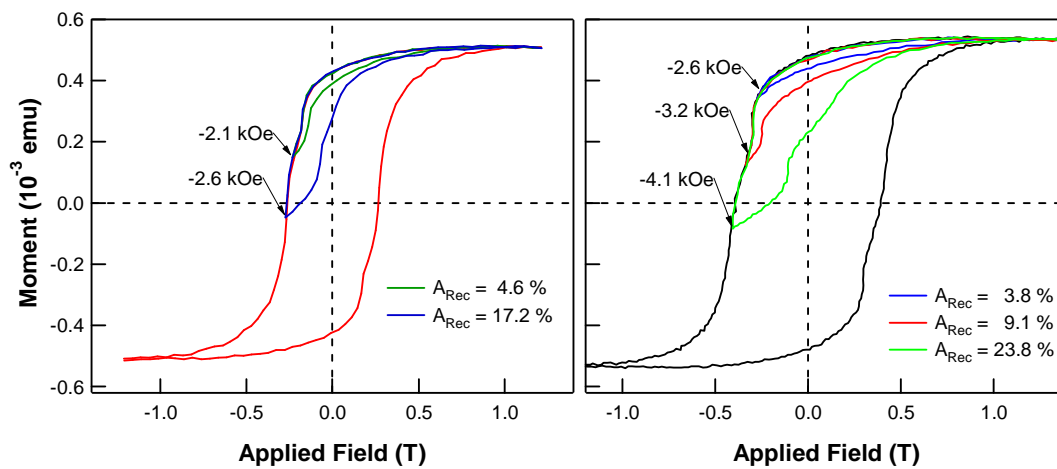


Fig. 3: Normalized recoil curves at 0 degree (in-plane) and 90 degree (out-of-plane). Reduced normalized recoil area in the out-of-plane curves is due to the higher out-of-plane coercive field in the CFO layer.

this improvement. Even for a much higher recoil field value of -3.2 kOe, the fraction of normalized area in out-of-plane orientation is much less than that of the in-plane orientation. This is in good agreement with the angle dependent measurements where the out-of-plane measurement show higher exchange spring, perhaps because that is the preferred direction of the moments induced by the soft magnetic layer's preferred direction.

It has been reported that the degree of exchange spring may be system dependent. For instance, in Ref. [9] it was reported the existence unavoidable hysteretic recoil curve for Co based system that can not be reduced, even though the field of irreversible switch, H_{irr} , is well past the coercive field. Our work, however, shows that indeed that area can be reduced.

One way to reduce the energy loss in the recoil curve is to introduce anisotropy, a preferred direction magnetic orientation by applying magnetic field during the deposition. With its water cooled magnet, our deposition system is uniquely equipped to provide the magnetic field during deposition needed to introduce this preferred direction. The approach we took was to apply magnetic field to the soft magnetic layer during deposition. The coercive field of the soft layer ($H_C < 100$ Oe at room temperature) is well within the field range accessible in our deposition system. To further enhance the introduced ordering and preferred direction, the field was maintained during cool down from 400°C to room temperature.

During typical deposition sessions, the substrates are rotated in order to achieve uniformity in the sputter deposited films by reducing shadow effect due to geometry and orientation of the source. However, to apply magnetic field so as to introduce ordering, the sample holder must not be rotated. In our system, to preserve uniformity while introducing preferred orientation, the first half of the soft magnetic layer was deposited with applied field in one direction and the other half was deposited with the field reversed by 180°.

Fig. 4 shows in-plane and out-of-plane exchange spring measurements on CFO/CoFe₂/CFO trilayer deposited. In this particular sample, the soft magnetic layer,

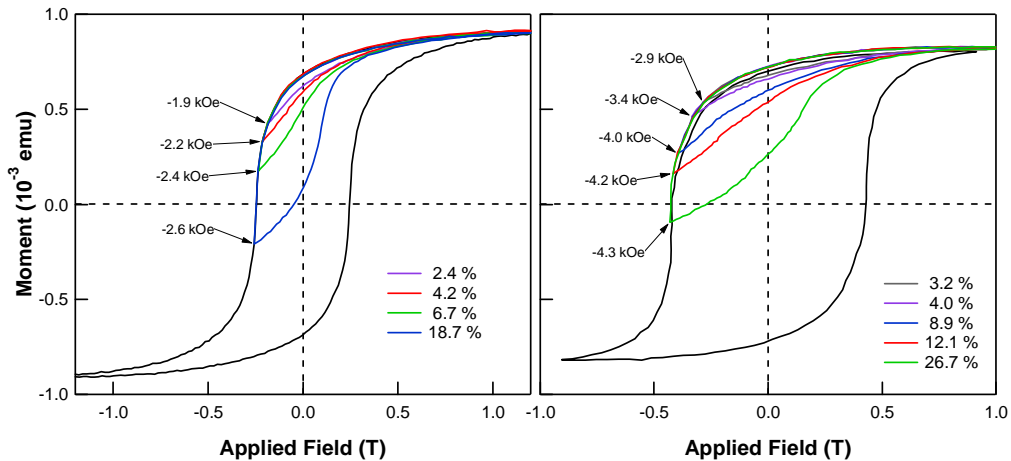


Fig. 4: Recoil curves of $\text{CoFe}_2\text{O}_4/\text{CoFe}_2/\text{CoFe}_2\text{O}_4$ trilayer where the CoFe_2 layer was deposited in applied field.

CoFe_2 , was deposited in an applied magnetic field. This trilayer will be referred to as in-field and the trilayer with CoFe_2 deposited with no applied field will be referred to as no-field. The first thing we observe is the consistency of the coercive field in both in case with no-field trilayer (**Fig. 3**) and in-applied trilayer (**Fig. 4**) at 2.6 kOe and 4.2 kOe for in-plane and out-of-plane directions, respectively. Moreover, in both cases, when the recoil field is greater than the coercive field, a substantial increase in the normalized recoil area is observed. This increase shows that the point of irreversible switching (H_{irr}) was crossed.

A closer examination of the curves, however, reveals the impact of the applied field during the deposition of the soft magnetic layer. Comparison of the curves reveals distinct recoil characteristics between the no-field trilayer and the in-field trilayer. In the case of the no-field trilayer, the signature of two-phase system is evident. This is marked by the initial switch in the magnetization followed by a sharp rise in the return path from H_{Rec} . This indicates a weak coupling between the soft and hard magnetic layer. In the case of the in-field trilayer, there is no trace of separate switching. Moreover, even at a higher recoil field value of -2.2 kOe, the normalized recoil area for the trilayer with CoFe_2 deposited in applied field (**Fig. 4: Left**), with 4.2% is smaller than 4.6% of the no-field trilayer at H_{Rec} of -2.1 kOe (**Fig. 3: Left**).

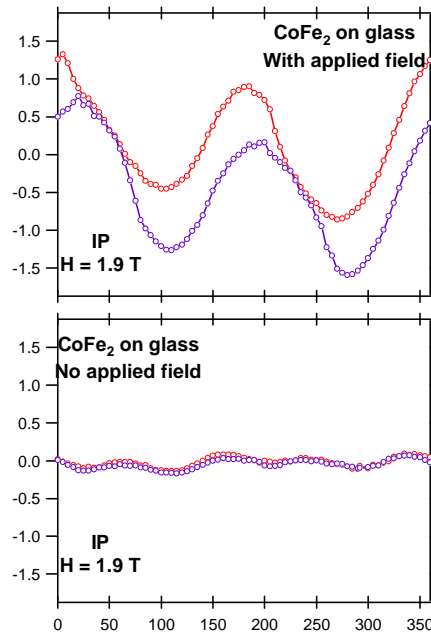


Fig. 5: Torque magnetometry for CoFe₂ film deposited on amorphous glass substrate with applied field and with no applied field. An in-plane uniaxial anisotropy is induced in the CoFe₂ due to the applied field.

In the case of out-of-plane direction, the difference is more remarkable. At H_{Rec} of -2.9 for in-field trilayer, the normalized recoil area is 3.2 % (**Fig. 4: Right**) to that of 3.8% at H_{Rec} of -2.6 kOe (**Fig. 3: Right**). This difference is, however, dwarfed close to the coercive field values. For the no-field trilayer, at H_{Rec} of -4.1%, the normalized recoil area is 23.8%, whereas for the in-field trilayer, with 12.1% it is half of that of the no-field trilayer at -4.2 kOe value of recoil field.

To explore the impact of the in-field deposition of the soft magnetic layer followed by in-field cooling trilayer structure, we performed the measurements listed below. A thick layer of CoFe₂, the soft magnetic layer was in-field deposited. To rule out contribution from the substrate, we chose an amorphous substrate, glass. The first measurement was done with on a 250 nm thick CoFe₂ layer deposited with no applied magnetic field. As expected, angle-dependent hysteresis measurements showed no anisotropy. This was also confirmed by torque magnetometry measurements done at 1.9 T (see **Fig. 5: bottom**). For the CoFe₂ deposited in an applied field, however, we observed angle dependence in the hysteresis loops. This result was confirmed by torque

magnetometry measurement shown in **Fig. 5: Top**. The result shows the induced uniaxial anisotropy in the soft magnetic layer deposited in an amorphous substrate.

As the result indicates, the cumulative contribution of the improvements in the coercive field and the induced anisotropy in the soft magnetic layer enhanced the exchange spring in the CFO/CoFe₂/CFO trilayers we are expanding our studies to include multiple trilayers. To this end we have started the modification of our UHV Pulsed Laser Deposition system to facilitate the sputtering of CoFe₂. Previously, we sputtered the CFO/CoFe₂/CFO trilayers however because of the inordinate time required to sputter the cobalt ferrite (five hours per layer), we decided to use the modified UHV Pulsed Laser Deposition system for the deposition of the multiple tri layered structures. We recently received instrumentation for the modification and should be commencing the work shortly.

3.1.3 REPORT ON LOW TEMPERATURE STUDIES

3.1.4 REPORT ON THE IMPACT OF NEW INSTRUMENTATION

3.1.5 Summary

We report exchange spring in sputter deposited trilayers of CoFe₂O₄/CoFe₂/CoFe₂O₄. Depositing the ferrimagnetic hard layer CFO in the presence of oxygen enhanced coercive field. We found the ratio of 7:1 of Ar to oxygen yielded the highest coercive field, whereas overabundance of oxygen during deposition had an adverse effect. Using recoil curve measurements, we showed that the improvement in the coercive field of the trilayer resulted in a pronounced exchange spring effect. As indicated by the analysis methodology we developed to quantify the degree of exchange spring, doubling the coercive field (from 2.6 to 4.1 kOe), reduced the recoil energy loss (from 4.6 to 3.8) in exchange spring by 20%. We also show that the energy loss in the exchange spring can be further reduced by introducing preferred direction for the moments of the soft magnetic layer. By depositing the soft magnetic layer in the presence of applied magnetic field, we were able to further reduce the energy loss by about 17% (from 3.8 to 3.2 at recoil field of -2.9 kOe). Our results show that applying magnetic field

during deposition and annealing induces magnetic anisotropy and enhances the coupling
 255 between the soft and hard magnetic layers improving the exchange spring.

3.1.6 References

1. T. Fix, S. Colis, K. Sauvet, J. L. Loison, G. Versini, G. Pourroy and A. Dinia, *Exchange coupling in NiO/CoFe₂ and CoFe₂O₄/CoFe₂ systems grown by pulsed laser deposition*, J. Appl. Phys. **99**, 043907 (2006).
- 260 2. E. F. Kneller and R. Hawig, *The exchange-spring magnet: A new material principle for permanent magnets*, IEEE Trans. Magn. **27**, 3588 (1991).
3. M. J. Carey, S. Maat, P. M. Rice, R. F. C. Farrow, R. F. Marks, A. Kellock, P. Nguyen and B. A. Gurney, *Spin valves using insulating cobalt ferrite exchange-spring pinning layers*, Appl. Phys. Lett. **81**, 1044 (2002).
- 265 4. A. Lisfi, C. M. Williams, L. T. Nguyen, J. C. Lodder, A. Coleman, H. Corcoran, A. Johnson, P. Change, A. Kumar, and W. Morgan, *Reorientation of magnetic anisotropy in epitaxial cobalt ferrite thin films*, Phys. Rev. B **76**, 054405 (2007).
5. J-P Zhou, H-C He, and C-W Nan, *Effects of substrate temperature and oxygen pressure on the magnetic properties and structures of CoFe₂O₄ thin films prepared by pulsed-laser deposition*, Appl. Surf. Sci. **235**, 7456 (2007).
- 270 6. A. Raghunathan, I. C. Nlebedim, D. C. Jiles, and J. E. Snyder, *Growth of crystalline cobalt ferrite thin films at lower temperatures using pulsed-laser deposition technique*, J. Appl. Phys. **107**, 09A516 (2010).
7. J-G Lee, K. Pyo Chae and J. Chul Sur, *Surface morphology and magnetic properties of CoFe₂O₄ thin films grown by a RF magnetron sputtering method*, J. Magn. Magn. Mater. **267**, 161 (2003)
- 275 8. X. S. Gao, D. H. Bao, B. Birajdar, T. Habisreuther, R. Mattheis, M. A. Schubert, M. Alexe and D. Hesse, *Switching of magnetic anisotropy in epitaxial CoFe₂O₄ thin films induced by SrRuO₃ buffer layer*, J. Phys. D: Appl. Phys. **42**, 175006 (2009).
9. E. E. Fullerton, J.S. Jiang, and S.D. Bader, *Hard/soft magnetic hetrostructures: model exchange-spring magnets*, J. Magn. Magn. Mater. **200**, 392 (1999)
- 280

3.2 *Fe/NWCNTS/SiO₂ and Nano Films of Fe on MgO*

3.2.1 Introduction

Nanowires of Fe were grown using magnetron DC sputtering in the lumens of carbon nanotubes vertically grown on SiO₂ substrate. Nanometric films of Fe on MgO(100) were synthesized at several deposition temperatures using magnetron DC sputtering. All samples were capped with Cu at room temperature without breaking vacuum to deter oxidation. Samples were studied using x-ray diffraction, vibrating sample magnetometer (VSM), torque magnetometer (TMM), and magneto-optic Kerr effect (MOKE). The system, Fe/MgO(100), despite its simplicity is family of systems that reveal unique properties with attractive effects for technological applications, such as giant and tunneling magneto-resistance [1- 5] as well as antiferromagnetic [6], oscillatory [7], and biquadratic exchange [8] couplings. Nanometric ultrathin films exhibit an out-of-plane uniaxial surface anisotropy sufficient to overcome demagnetizing field [1]. This feature is important for higher density magnetic media. This system in addition to its enormous potential for technological applications it is an attractive research object in nanomagnetism [9]. The substrate MgO is an ideal substrate to grow quasi free standing metal structures on which effects of reduced dimensionality of metal can be studied because of the very weak interaction between Fe and MgO predicted theoretically by full-potential linearized augmented-plane-wave-total-energy method [10] and demonstrated experimentally by x-ray photoelectron spectroscopy (XPS) and x-ray absorption spectroscopy (XAS) showing the interface between Fe(001) and MgO(100) to be stable for temperatures up to 670 K [11].

The importance of Fe/MgO system is also demonstrated by the several experimental and theoretical studies on Fe/MgO (100) nanometric films [10 - 25]. Ab-initio calculations yielded optimistic TMR ratio in excess of 100% [12] for Fe/MgO/Fe. XAS and photoemission experiments observed changes in 3d band due to evolution of Fe local atoms coordination from a bulk-like situation to a configuration where low dimensionality effects are significant [13]. Salvador et al [14] showed that for uncapped nanometric ultra thin films of Fe, the magneto-crystalline anisotropy of the films increased with deposition temperature indicating improved crystalline structures. Further

was shown the saturation value of the magneto-crystalline anisotropy (550 Oe corresponding to bulk Fe) was reached at a deposition temperature of 300 °C. Our study on nanometric ultra thin films of Fe/MgO(100) also showed saturation magnetization was a maximum at deposition temperature of 200 °C. Maximum coercive field occurred at 100 °C, Figure 2a, indicative of higher magneto-crystalline anisotropy. The coercive field showed a large decrease at deposition temperatures of 200 °C and 300 °C. This corresponds with the appearance of secondary Fe (200) peak at $\theta = 65^\circ$ in the XRD for samples deposited at these two high temperatures. The primary peak Fe (200) peak for all planar film samples occurred at $\theta = 44.5^\circ$, Fig. 1.

Density functional calculations have shown, application of electric field have significant effect on the interface magneto-crystalline anisotropy. This is due to change in relative occupancy of 3d-orbitals of Fe atoms on Fe/MgO interface. This suggests possible application of Fe/MgO systems for electrically controlled magnetic data storage, multi-ferroic device [15].

In this study structural and magnetic properties of nano-metric Fe thin films on MgO(100) and nano wires of Fe prepared in the lumens of MWCNTs using magnetron DC-sputtering were studied using XRD, VSM, TMM, and MOKE measurements. Magnetic measurements using VSM showed that samples prepared at 100 °C exhibit the highest coercive field ($H_C = 176$ Oe) while samples prepared at 50 °C show high remnant magnetization ($M_r = 119$ emu/g) and samples prepared at 200 °C show the highest saturation magnetization ($M_s = 147$ emu/g), which is 68% the saturation field of bulk Fe measured by absolutely force method at room temperature [20]. As shown in Table 1 the three parameters extracted from a B-H loop H_c , M_r , and M_s are at their maximum values at different substrate growth temperatures. In our study nanowires of Fe capped with Cu in the lumens of MWCNTs vertically grown on SiO_2 exhibited an enhanced magnetic property of 137 Oe coercivity. This result is comparable with our recent result of single walled carbon nanotubes coated with Fe_2O_3 nanoparticles [26] and exceeds that of graphene coated with Fe_2O_3 nanoparticles [27].

3.2.2 Experiment

Vertically aligned MWCNTs were filled with Fe and capped with Cu in this experiment were grown using a thermal CVD method [28] on SiO₂ substrate. This method involves exposing silica structures to a mixture of ferrocene and xylene at 770 °C for 10 min. The furnace is pumped down to ~200 mTorr in argon bleed and then heated to the temperature of 770 °C. The solution of ferrocene dissolved in xylene (~0.01g/ml) is pre-heated in a bubbler to 175 °C and then passed through the tube furnace. The furnace is then cooled down to room temperature. The open ended MWCNTs tips were filled with Fe and capped with Cu using DC magnetron sputtering method at a substrate temperature of 100 °C. Substrate temperature CNTs was chosen since a planar sample grown at this substrate temperature exhibited the highest value of coercive field amongst all planar films grown at several other substrate temperatures as shown in Fig. 2(a).

Nano-metric thin films epitaxially grown on MgO (100) substrate (5mm X 5mm X 50 µm) (from MTI company) using magnetron DC sputtering (AXXIS tool from K. J. Lesker company) at several temperatures. All substrates were degassed at 350 °C in vacuum of 0.1 micro Torr for 1800 s and samples were pre and post annealed at the deposition temperatures for 1800 S in vacuum. All samples were capped with 5 nm of Cu to deter oxidation after cooling the sample down to 20 °C. The source substrate distance was kept fixed at 30 cm and the substrate was kept at 45° while, being rotated at a constant rate of 20 rpm for uniform deposition. With these condition epitaxial Fe grow on MgO (100) due to a good lattice match of MgO ($a=4.213 \text{ \AA}$) and Fe ($a=2.866 \text{ \AA}$) and weak interface interaction [10, 11] free standing Fe is formed. The 45° in-plane rotation of the substrate during deposition provides the growth of an even surface. The deposition rate for Fe was 0.17nm/s, as calibrated by deposition time versus thickness measurements for Fe films several hundred thick.

XRD measurements were carried out using Rigaku D/Max Ultima II instrument: x-ray of 40kV, 40 mA, Cu K α , div. slit of 1 deg, div. H.L. slit of 5 mm, sct. slit of 0.6 mm, rec. slit of 0.6 mm, scan speed of 2.0 deg./min, scan mode of continuous, sampling width of 0.02, and geometry θ -2 θ .

Fig. 2(a) depicts coercive field (H_c), saturation and remnant magnetization (M_s & M_R) Vs temperature for planar Fe/MgO films as well as nano-wire of Fe/MWCNTs. Fig. 2(b) VSM measurements of M Vs H for samples synthesized at several substrate temperatures. In Fig. 2(c) and Fig. 2(d) M Vs H loops of planar film and wire synthesized at 100 °C substrate temperature at several angles between the applied field and normal to the surface.

Fig. 3(a) depicts torque magnetometer measurements at an applied magnetic field of 20 kOe of samples synthesized at several substrate temperatures. In Fig. 3(b) MOKE measurements is presented in polar plots. Hysteresis loops were measured using MOKE in longitudinal configuration, from the recoded hysteresis loop the coercive fields of samples were measured as a function of angular position of the sample relative to the applied magnetic field direction, Fig. 3b. The operating principles of MOKE consist of measuring changes in polarization of light reflected from magnetic sample. The MOKE setup consists of a monochromatic light source (HeNe laser, 632 nm wavelength and 5 mW output power), polarizer, analyzer, photodiode, electromagnet, lock-in amplifier, pre-amplifier and an optical chopper or photoelastic modulator. The reflected beam from a magnetic sample is passed through a second polarizer which is the analyzer in order to select the component of the E -field perpendicular to the plane of incidence. This will make the normalized intensity detected proportional to the component of the magnetization of the sample parallel to the applied magnetic field.

Fig. 3(c) and Fig. 3(d) show torque magnetometer measurements of planar film of Fe/MgO(100) and nano wire of Fe/MWCNTs synthesized at 100 °C.

3.2.3 Results and Discussions

It is well known that structural property is important in magnetism [1]. For this reason one of the goals of this study is to correlate the structure of films to their magnetic property. The structures were characterized by x-ray diffraction using $\text{CuK}\alpha$ radiation. As shown in Figure 1 XRD indicates that an extra Fe(200) peak is present at higher deposition temperature this can be explained qualitatively as follows, an Fe atom

reaching the substrate at an arbitrary site will not stay at that site for deposition temperature high enough. It will have enough thermal energy to move to an appropriate site to form a crystalline structure. Even though XRD of the film deposited at 100 °C does not show a peak at Fe (200), it possesses a maximum coercive field as shown in Figure 2(a).

On the other hand as shown in Table 1 and Fig 2(a) the remnant and saturation magnetizations are minima at growth temperature of 100 °C. The saturation

T (°C)	H _c (Oe)	M _s (emu/g)	M _R (emu/g)	S= M _R /M _S
50	103	132	119	0.906
100	176	91.8	76.4	0.832
200	41.6	147	104	0.707
300	8.30	122	94.6	0.773

Table 1: Magnetization values of Magnetization values of Fe grown on MgO(100) by magnetron DC sputtering at several deposition temperatures. Measurements were taken using VSM at room temperature.

magnetization, M_s has a maximum value for films deposited at 200 °C for which the coercive field is a minimum. The squareness S=M_R/M_S has a minimum value for films grown at this deposition temperature. This variation is depicted in Figure 2(b) where

Angle	H _c (Oe)		M _s (emu/g)		M _r (emu/g)	
	Film	Nano-Wire	Film	Nano-Wire	Film	Nano-Wire
0	176	137	91.8	38	76.4	27
45	243	115	57.9	35	46.2	24
90	179	59.8	13.2	28	88.6	19

Table 2: Magnetization values of Fe/MgO(100) film and Fe/MWCNTs/SiO₂ nano-wires deposited at 100o C by magnetron DC sputtering at several angles between the applied magnetic field and the surface normal. Measurements were taken using hysteresis loops for the various Fe/MgO(100) film prepared at several deposition temperatures measured using VSM at room temperature. For the sample with the highest value of H_c, Figure 2(c) depicts, hysteresis loops for various orientation of the magnetic field with the surface normal for Fe / MgO(100) film prepared at 100 °C measured using VSM at room temperature. The in-plane at 0° between the applied field and the surface of the sample and the out of plane hysteresis loops are similar as shown in Figure 2(c), indicating that the easy axis is in-plane where as the hard axis is perpendicular to the sample's plane. In Table 2 values of H_c, M_s, and M_r for Fe/MgO(100) planar film and

wires Fe/MWCNTs deposited at 100 °C are listed as shown in the data H_c was a maximum at 45° and M_r and M_s were minimum.

On the other hand M_r and M_s were at their maxima and H_c at its minimum at 0° and at out-of plane orientation. This is another indication that the easy magnetization axis lie in plane and the hard axis out of plane. Seifu et al [29] showed that the hysteresis loop of Fe-filled MWCNTs exhibits an anomalous narrowing of the loop at the zero magnetization axes. Lopez-Urias, et al [25] reported formation of helical spin configurations during magnetization of ferromagnetic nanowires encapsulated inside carbon nanotubes.

Maximum coercive field of 176 Oe was observed at synthesis temperature of 100 °C for films and 137 Oe for nanowires, a maximum remnant magnetization of $M_r=120.0$ emu/g was observed at 50 °C, a maximum saturation magnetization of $M_s=146.4$ emu/g was observed at 200 °C, and the squareness defined $S= M_r/M_s$ was 80% for 2D films and 70% for 1D wire.

MOKE data indicates the coercive field is a maximum for samples with growth temperature of 100 °C in agreement with VSM. The magnetic torque curve, Figure 3, indicates pronounced 2 fold magnetic symmetry at higher deposition temperature. The torque curve in Figure 3(a) for sample prepared at 100 °C shows less pronounced two-fold symmetry compared to torque curve of samples prepared at higher substrate temperatures. In Figure 3(c) the 100 °C sample shows comparatively higher pronounced at 20 kOe than at lower field strengths there is a transition between 1 kOe and 5 kOe. Figure 3(c) and 3(d) depict 100 °C synthesized thin film and nano-wire at several applied fields. Both show similar trend except at low fields the loop for nano-wire is off center. Figure 3(b) depicts that the ____ of thin films surfaces do not show two-fold symmetry.

3.2.4 Conclusion

In conclusion we have synthesized Cu capped Fe/MgO(100) nanometric thin films and Cu capped nanowires of Fe using MWCNTs as templates. Nanowires were grown at an optimized condition set by growing planar films at several deposition temperatures that showed the best magneto-crystalline property. Magnetic measurements

445 showed that nanowires exhibited higher anisotropy requiring higher saturation field compared to planar thin films due to magnetic shape anisotropy however, similar magnetic symmetry, two-fold, was observed in nano-metric films and wires. The squareness of nanowires is by 10% less than planar nanometric thin films.

450 3.2.5 References

1. B. Heinrich and J.A.C. Bland (ed) Ultrathin Magnetic Structures. (Berlin: Springer 1994).
2. S. Yuasa, T. Nagahama, A. Fukushima¹, Y. Suzuki, and K. Ando, *Nature*, **3**, 868 (2004).
- 455 3. D. D. Djayaprawira, K. Tsunekawa, M. Nagai, H. Maehara, S. Yamagata, and N. Watanabe, S. Yuasa, Y. Suzuki, and K. Ando, *APPLIED PHYSICS LETTERS* **86**, 092502 (2005)
4. S. Yuasa, A. Fukushima, T. Nagahama, K. Ando, and Y. Suzuki, *Japanese Journal of Applied Physics*, **43**, 4B, 2004, L 588–L 590 (2004)
- 460 5. M. Bowen, V. Cros, F. Petroff, and A. Fert, C. Martí'nez Boubeta, J. L. Costa-Kra'mer, J. V. Anguita, A. Cebollada, and F. Briones, J. M. de Teresa, L. Morelló'n, and M. R. Ibarra, F. Gu'ell, F. Peiro', and A. Cornet, *Applied Physics Letters* **79**, 1655 (2001).
6. P. Grunberg, R. Schreiber, Y. PangM. B. Brodsky, H. Sowers, *PHYSICAL REVIEW LETTERS*, **57s**, 19 (1986).
- 465 7. S. S. P. Parkin, N. More, and K. P. Roche, *PHYSICAL REVIEW LETTERS*, **64**, 19 (1990).
8. M. Ruhrig, R. Schafer, A. Hubekt, R. Mosler, J. A. Wolf, S. Demokrlrov, and P. Grunrer, *phys. stat. sol. (a)* **125**, 635 (1991)
- 470 9. S. D. Bader, *Reviews of Mod. Phys.*, **78**, 1 (2006).
10. C. Li, A. J. Freeman, *Phys. Rev. B*, **43**, 780 (1991).
11. P. Luches, S. Benedetti, M. Liberati, F. Boscherini, I. I. Pornin, and S. Valeri, *Surf. Sci.* **583**, 191 (2005).
12. J. Mathon and A. Umerski, *Phys. Rev. B*, **63**, 220403 (2001).
- 475 13. P. Luches, P. Torelli, S. Benedetti, E. Ferramola, R. Gotter, S. Valeri, *Surf. Sci.* **601**, 3902 (2007).
14. C. Salvador¹, T. Freire¹, C. G. Bezerra¹, C. Chesman¹, E. A. Soares, R. Paniago, E. Silva-Pinto, and B. R. A. Neves, *J. Phys. D: Appl. Phys.* **41** (2008).
- 480 15. M. K. Niranjan, C. G. Duan, S. S. Jaswal, E. Y. Tsymbal, *Applied Physics Letters*, **96** (2010).
16. C. M. Boubeta, C. Clavero, J. M. García-Martín, G. Armelles, A. Cebollada, Ll. Balcells, J. L. Menéndez, F. Peiró, A. Cornet, and Michael F. Toney, *Phys. Rev. B*, **71**, 014407 (2005).
- 485 17. J. Balogh, I. Dézsi, Cs. Fetzner, J. Korecki, A. Koziół-Rachwał, E. Młyńczak, and A. Nakanishi. *Phys. Rev. B*, **87**, 174415 (2013).
18. S. Yang, H. K. Park, J. S. Kim, J. Y. Kim, and B. G. Park, *J. Appl. Phys.* **110**, 9 (2011).
19. J.L. Costa-Kramer, J.L. Menéndez, A. Cebollada, F. Briones, D. Garcia, A. Hernandez, *J. Magn. Magn. Mater.*, **210**, 341–348 (2000).
- 490 20. J. Crangle and G. M. Goodman, *Proc. Roy. Soc. A.*, **321**, 477 (1971).
21. H. Fuke, A. Sawabe, and T. Mizoguchi, *Jpn. J. Appl. Phys.*, **32** (1993).
22. K. Postava, J.F. Bobo, M.D. Ortega, B. Raquet, H. Ja'eres, E. Snoeck, M. Goiran, A.R. Fert, J.P. Redoules, J. Pistora, J.C. Ousset, *J. Magn. Magn. Mater.* **163**, 8 (1996).

23. G. Schütz, W. Wagner, W. Wilhelm, P. Kienle, R. Zeller, R. Frahm, and G. Materlik, *Phys. Rev. Lett.* **58**, 7, 1987.
24. B. Sinković, P. D. Johnson, N. B. Brookes, A. Clarke, and N. V. Smith, *Phys. Rev. Lett.* **65**, 1647 (1990).
25. F. López-Urías, E. Muñoz-Sandoval, M. Reyes-Reyes, A. H. Romero, M. Terrones, and J. L. Morán-López, *Phys. Rev. Lett.*, **94**, 216102 (2005).
26. S. Neupane, S. Khatiwada, C. Jaye, D. Fisher, H. Younes, H. Hong, S. Karna, S. Hirsch, and D. Seifu, *ECS J. of Solid State Science and Tech.*, **3** (8) M39-M44, 2014.
27. S. Neupane, H. Hong, L. Giri, S.P. Karna, and D. Seifu, *J. of Nanoscience and Nanotechnology*, Vol. 15, 1-5, 2015.
28. B. Q. Wei, R. Vajtai, Y. Jung, J. Ward, R. Zhang, G. Ramanath, and P. M. Ajayan, *Chem. Mater.*, **15**, 1598-1606, 2003.
29. Percy Szalkowski (ed), *Carbon Nanotubes: Select Army Research Laboratory Studies*, Chapter 4, (NOVA 2013).

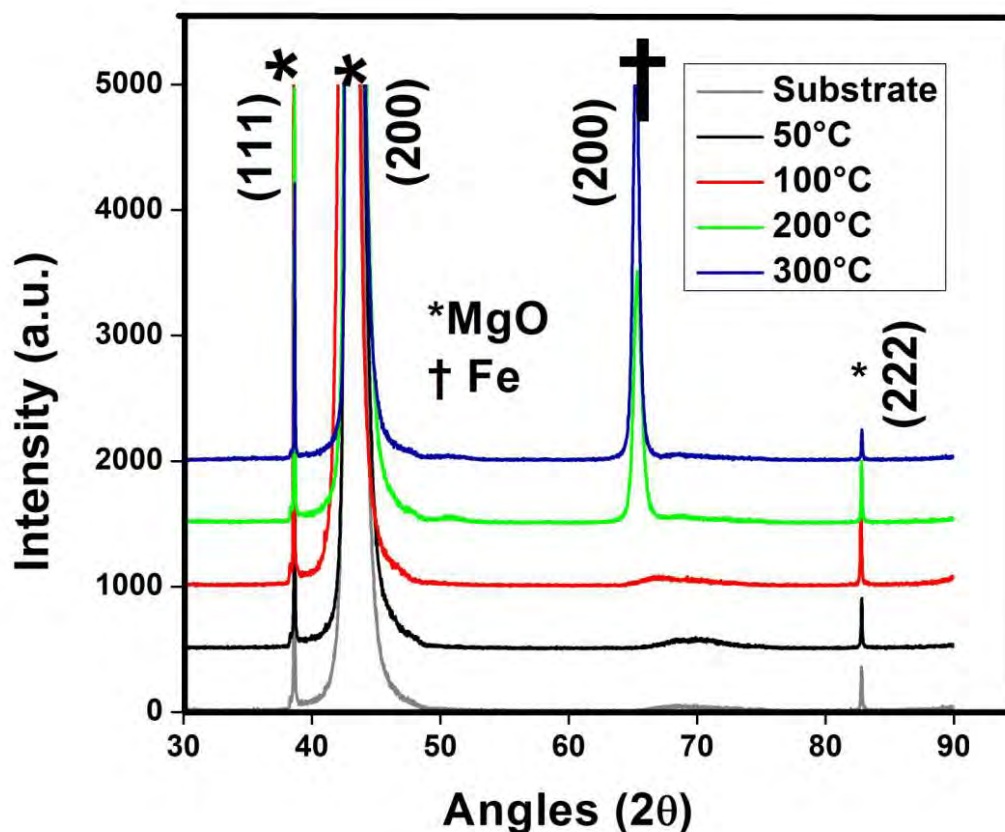


FIG. 1: XRD patterns of Fe/MgO(100) at various growth temperatures. The insert is a zoom in at the Fe Bragg peak.

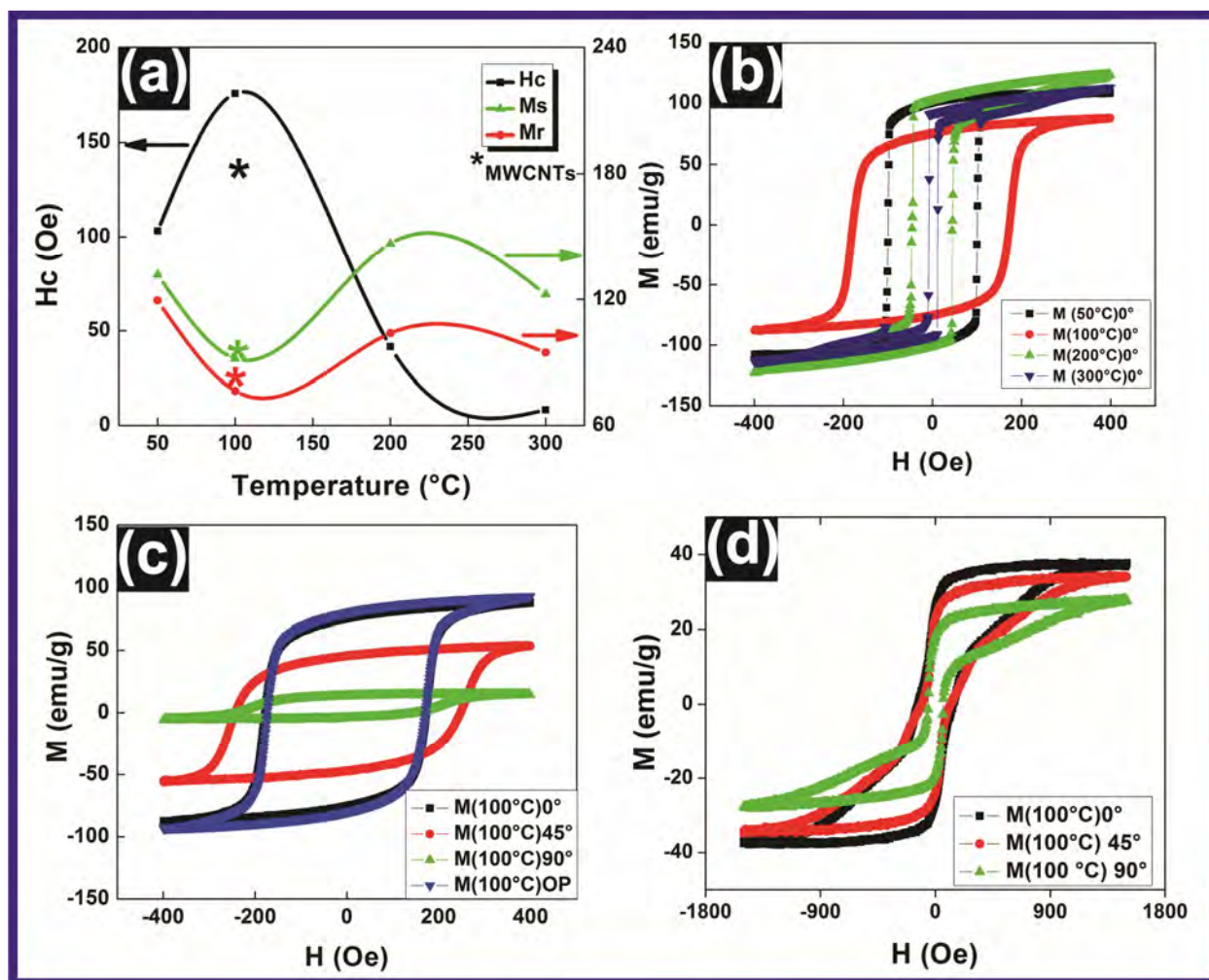


Figure 2. (a) Coercive field Vs growth temperature of Fe/MgO(100) measured with VSM. Coercive field of Fe/MWCNTs nano-wires synthesized at 100 °C indicated by '*'.
 (b) Magnetic hysteresis loops for Fe/MgO(100) films for various growth temperatures as measured by VSM at room temperature. All loops are measured out of plane with the applied field perpendicular to the normal vector to the sample's surface $\theta=0^\circ$.
 (c) Magnetic hysteresis loops for Fe/MgO(100) film prepared at 100 °C at various angles between the normal vector to the surface and the applied magnetic field. The purple loop is for out of plane (OP) measurement $\theta=0^\circ$.
 (d) Magnetic hysteresis loops for Fe/MWCNT wire prepared at 100 °C at various angles between the normal vector to the sample's surface and the applied magnetic field.

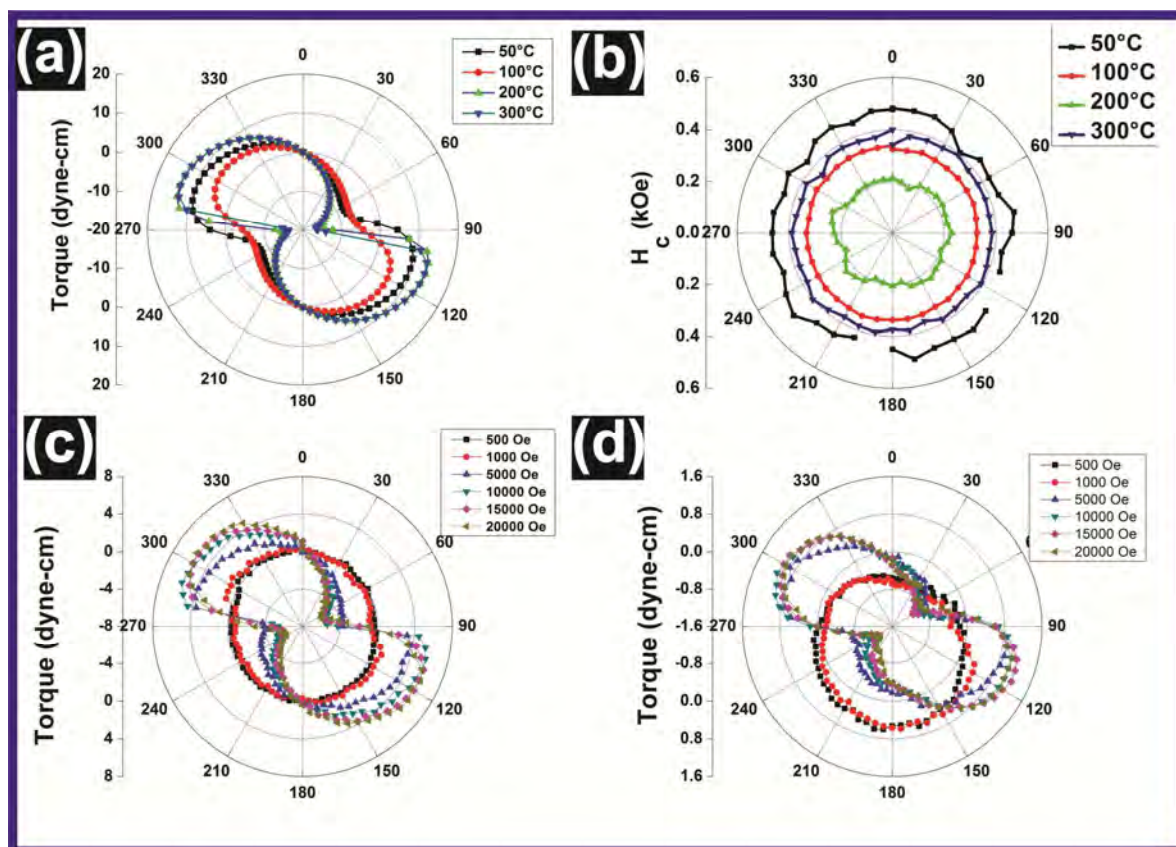


Figure 3. (a) Magnetic torque curves of Fe / MgO(100) films for various growth temperatures at room temperature measured at an applied field of 20kOe.

(b) Magneto-optical longitudinal Kerr loops of Fe / MgO(100) films for various growth temperatures at room temperature.

(c) Magnetic torque curves of Fe / MgO(100) films at growth temperature of 100 °C measured at several applied fields at room temperature measured.

(d) Magnetic torque curves of Fe / MWCNTs wires at growth temperature of 100 °C measured at several applied fields at room temperature measured.

4 Student Contributions

A number of students worked at different times and different parts of the project. The students were Jaime Arribas, Dominic Smith and Keion Howard. One of their main tasks was to assist in the synthesis of multilayer exchange spring samples using the sputtering DCA-450 and subsequent characterization of the samples. In order to perform these tasks safely, the students were trained and supervised. For their work, they were granted access to resources available in the labs and given hands-on training on all equipments and

discussions on safe and best practices. All students took part in fabricating and
 550 characterizing exchange spring samples. The tasks include (1) cutting, cleaning and
 mounting substrates for deposition in the DCA-450's load-lock chamber; (2) fabricate the
 sample with the designed composition and structure under the specified conditions; (3)
 characterize the sample following fabrication using the equipments available in the lab be
 it VSM, torque magnetometer or measure its thickness using the Profilo-meter; and (4)
 555 analyze the data which in turn lead to further measurements. As they gained experience
 and understanding of the process, the students actively participated in the design and
 analysis of the next set of experiments.

In addition to the above stated tasks, the students were given access to resources such
 as the machine shop and scientific equipments that can be computer-controlled. This was
 560 to empower them to explore and discover on their own by working on areas in the project
 they identified. In the end, each student made a unique contribution to the project in his
 way. Enumerated below are individual contributions.

4.1 Jaime Arribas

Being the first student to work on the research, student Jaime Arribas contributed
 565 immensely in bringing the different equipments online and ready for depositing thin
 magnetic films. In the process he worked on and had the diamond saw ready for cutting
 glass substrates for the deposition of thin films. After cutting the glass substrate to the
 desired dimensions of 5x5 mm or 10x10 mm, he cleaned the substrates for introduction
 into the sputtering deposition system.

Mr. Arribas took part in putting together a magneto-resistance measurement station
 570 and developing the LabView based control and data acquisition software. This gave him
 a chance to learn the programming language that utilizes symbols and wires to design a
 control system. To do that, however, he needed to learn the instrument communication
 protocols and explored at length the writing and debugging processes. Mr. Arribas
 575 presented his work at the Morgan Innovation Day in Annapolis, MD and was featured in
 a subsequent Radio interview by WEAA. The next summer, when he went to NASA
 summer internship, he said the exposure and experience proved of great use. He

attributed his fluency of the LabView code he learned while working on this project and thus was able to develop the requested code with greater ease and efficiency.

580 He also paved the way for the other students who followed him by providing guidance and sharing the challenges he had and ways he overcome those challenges.

4.2 Dominic Smith

Mr. Smith developed a Python code for real-time data visualization and analysis. Just
585 by himself, he learned the modeling and computer assisted design (CAD) software called SolidWork. Using that modeling package, he was able to design and 3D render the items which were then machined using the CNC Milling machine available in the machine shop.

4.3 Keion Howard

Howard was a very insightful student who was able to improve and come up with
590 straightforward procedures for loading the samples and maintain the equipments in the lab. With his remarkable grasp of 3D positioning and placement of objects in the vacuum chambers, he quickly mastered the sample transfer from the load-lock to the main chamber and back. He then went on to simplified the sample transfer task into a clear procedural steps, when followed properly resulted in very repeatable and reliable transfer
595 of the sample to and from the main chamber. Mr. Howard also took part in conducting liquid nitrogen (LN2) temperature VSM measurements. With our Model 10 VSM setup, it is possible to go down to 80 K. The challenge is stabilizing the system at the desired temperature for it is sensitive to external factors. Mr. Howard quickly comprehended and intuitively mastered the intricate details of operating the system. With his patience and
600 systematic approach, he was able to perform reproducible measurements of the highest quality. Just before the end of his work, he was able to deposit trilayer CFO/CF/CFO sample on the DCA-450 sputtering system by himself.

4.4 Impact of the experience on the students

In broader sense, this first time introduction and exposure to research had great
605 impact on the students. It turned out to be a learning experience to the students in regards to the relevance to the work. The approach that we took was to get the students involved

in the task and process at hand so that they were exposed to the different equipments and resources that are available in the lab. At different times the focus of their involvement was such that it provided the students with experience on how research is conducted from
610 designing an experiment to preparing, synthesizing and characterizing the samples followed by interpreting the results.

In short, as can be inferred from the impact of this experience had on the students, it can be said that this opportunity demystified working in a research facility and made research accessible. It enabled them to view research as an extension of learning in class
615 and develop deeper appreciation for research and make their unique contribution.